THE JOURNAL OF BIOLOGICAL CHEMISTRY VOL. 289, NO. 10, pp. 6498–6512, March 7, 2014

Mechanism and Function of Monoclonal Antibodies Targeting Siglec-15 for Therapeutic Inhibition of Osteoclastic Bone Resorption*

Received for publication, November 8, 2013, and in revised form, January 16, 2014 Published, JBC Papers in Press, January 20, 2014, DOI 10.1074/jbc.M113.494542

Matthew Stuible, Anna Moraitis, Annie Fortin, Stefan Saragosa, Aida Kalbakji, Mario Filion, and Gilles B. Tremblay[1]
From Alethia Biotherapeutics Inc., Montréal, Québec H2X 1Y4, Canada

Background: Bone-resorbing osteoclasts express the Siglec-15 receptor on their plasma membrane.
Results: Siglec-15 antibodies inhibit osteoclast differentiation and induce receptor endocytosis and degradation.
Conclusion: These results establish that Siglec-15 antibodies target osteoclasts *in vivo* and reveal a likely mechanism of action.
Significance: Siglec-15 could serve as a target of novel therapeutics for osteoporosis and cancer-associated bone loss.

The use of monoclonal antibodies to target functionally important cell-surface proteins on bone-resorbing osteoclasts represents a promising approach for treatment of cancer-associated bone loss and other skeletal pathologies. Previously, we identified Siglec-15, a little studied sialic acid-binding receptor, as a candidate target that is highly up-regulated during osteoclast differentiation induced by the cytokine receptor activator of NF-κB ligand (RANKL). In this report, we confirm that Siglec-15 is localized to the plasma membrane where it can be targeted by monoclonal antibodies to inhibit differentiation of functional osteoclasts *in vitro*. Furthermore, we found that treatment of mice with these antibodies led to a marked increase in bone mineral density, consistent with inhibition of osteoclast activity. Interestingly, osteoblast numbers were maintained despite the anti-resorptive activity. At the molecular level, Siglec-15 interacts with the adapter protein DAP12 and can induce Akt activation when clustered on the osteoclast cell surface, which likely represents its normal signaling function. Importantly, we discovered that monoclonal antibodies induce rapid internalization, lysosomal targeting, and degradation of Siglec-15 by inducing receptor dimerization. This study defines a key regulatory node that controls osteoclast differentiation and activity downstream of RANKL and supports further development of Siglec-15 antibodies as a novel class of bone loss therapeutics.

Skeletal homeostasis in adults requires the balanced activities of two critical cell types: bone-forming osteoblasts and bone-resorbing osteoclasts. Pathological conditions such as osteoporosis and cancer-associated bone loss involve a shift in this equilibrium to favor osteoclastic bone destruction. Osteoclasts differentiate from common monocyte/macrophage precursors in response to the critical cytokine receptor activator of NF-κB ligand (RANKL).[2] As the sole cells able to digest mineralized bone, multinucleated osteoclasts are functionally and morphologically unique. Thus, there is potential to identify proteins that are uniquely expressed on the osteoclast cell surface, in particular for development of highly targeted antibody-based therapeutics for bone loss (1).

Using the STAR subtractive cloning technology (2), we identified sialic acid binding immunoglobulin-like lectin-15 (Siglec-15) as an mRNA transcript highly up-regulated in mature osteoclasts compared with their non-differentiated precursor cells (3). The Siglecs are a family of type I transmembrane proteins that are distinguished by N-terminal immunoglobulin-like domains that bind to sialylated glycoconjugates and are typically expressed in subsets of hematopoietic cell types (4). We examined the importance of Siglec-15 in tissue culture models of osteoclastogenesis and found that RNAi-mediated knockdown of Siglec-15 expression impaired RANKL-induced differentiation of primary human osteoclast precursors (HOPs) and the mouse RAW264.7 cell line (3). A recent study reported the overexpression of Siglec-15 in giant cell tumors of the bone, which are characterized by abundant osteoclast-like cells, and in agreement with our results, the authors observed dramatic up-regulation of Siglec-15 mRNA in differentiating HOPs and RAW264.7 cells (5). The effect of Siglec-15 RNAi on osteoclast differentiation has since been independently confirmed in mouse bone marrow macrophages (6). Importantly, we also found that, besides osteoclasts, Siglec-15 mRNA expression is nearly absent from a panel of normal human tissues (3). Together, these results showed that Siglec-15 is an osteoclast-specific Siglec that could be targeted to inhibit bone resorption; thus, we proceeded to generate monoclonal antibodies against Siglec-15 that were tested as potential therapeutic candidates.

The Siglec receptors can influence intracellular signaling by two general mechanisms (7). First, the relatively short cytoplasmic domain found in several Siglecs contain immunoreceptor tyrosine-based inhibitory motifs (ITIMs), which can recruit phosphatases to inhibit cell signaling (8, 9). Second, certain Siglecs contain a distinctive positively charged residue within their transmembrane domains that can interact with the trans-

*All authors are current or former employees of Alethia Biotherapeutics.
[1] To whom correspondence should be addressed: 141 President Kennedy Ave., Suite SB-5100, Montréal, Québec H2X 1Y4, Canada. Tel.: 514-858-7666 (ext. 208); Fax: 514-858-5333; E-mail: gilles.tremblay@alethiabio.com.
[2] The abbreviations used are: RANKL, receptor activator of NF-κB ligand; Siglec-15, sialic acid binding immunoglobulin-like lectin-15; HOP, human osteoclast precursor; ITAM, immunoreceptor tyrosine-based activation motif; Fab, antigen binding fragments; TRAP, tartrate-resistant acid phosphatase.

membrane immunoreceptor tyrosine-based activation motif (ITAM)-bearing co-receptors, such as DAP12 (10, 11). DAP12 serves as a signaling module for a variety of immune receptors by recruiting the kinase Syk and other signaling molecules upon ligand binding to associated receptors (12, 13). Siglec-15 contains both a cytoplasmic ITAM as well as a lysine residue in its transmembrane region that permits interaction with DAP12 upon co-overexpression (14). This combination of activating and inhibitory motifs implies that the signaling effects of Siglec-15 are complex. However, a variety of studies have revealed the diverse cellular roles of other members of the Siglec family. These include the modulation of signaling through other immunoreceptors (*e.g.* CD22) (15), the formation of cell-cell contacts (*e.g.* sialoadhesin) (16), and possibly the recognition of sialic acid moieties on pathogens, similar to pattern-recognition receptors (*e.g.* Siglec-H) (17).

Here, we report that monoclonal antibodies targeting Siglec-15 effectively inhibit osteoclast activity *in vitro* and *in vivo*. We proceed to characterize the molecular function of the Siglec-15 protein in osteoclasts, including its expression, subcellular localization, and role in cell signaling. These studies reveal that DAP12-dependent signaling requires clustering of Siglec-15 on the osteoclast cell surface, whereas antibody-induced dimerization leads to its endocytic down-regulation. These findings have shed light on the mechanism of action of these candidate therapeutic antibodies.

EXPERIMENTAL PROCEDURES

Antibodies—Monoclonal antibodies against human Siglec-15 were generated using a phage-display technology (Alere San Diego, San Diego, CA). A library of antigen binding fragments (Fabs), expressed recombinantly in *Escherichia coli*, were screened by ELISA for Siglec-15 binding, and several individual clones with diverse immunoglobulin variable chain sequences were selected for further characterization. The heavy and light immunoglobulin chain variable regions of these Fabs were cloned into expression vectors encoding corresponding human immunoglobulin constant regions and full chimeric antibodies were produced by transient transfection of these constructs in 293-6E cells. Certain monoclonals, including E09 and B02, were subsequently subcloned into other vectors to express full mouse antibodies. Humanized forms of the Siglec-15 antibodies were also generated using a computational approach at the National Research Council Biotechnology Research Institute (Montreal, Quebec). All antibodies were purified from 293-6E supernatants by Protein A affinity chromatography; Protein A elution buffer (0.2 M glycine, pH 2.0) was exchanged for PBS prior to antibody storage. For the current study, we used chimeric forms of Siglec-15 antibodies E06 and E10, respectively, for all immunoprecipitation and Western blotting applications. The mouse form of B02 was used for the *in vivo* experiments, and humanized E09 and B02 were used, as indicated, for cell-based assays.

Other antibodies were purchased from Cell Signaling (monoclonal anti-ERK, monoclonal anti-phospho-ERK (Thr-202/Tyr-204), polyclonal anti-Akt, polyclonal anti-phospho-Akt (Ser-473)), U.S. Biological Corp. (polyclonal anti-mouse-DAP12) and the Developmental Studies Hybridoma Bank (monoclonal anti-LAMP2, clone GL2A7). Human and mouse IgG, used as non-targeting control antibodies, were from Innovative Research.

Cell Culture—For osteoclast differentiation, RAW264.7 cells (ATCC, Manassas, VA), grown in DMEM containing 10% fetal calf serum (Invitrogen) and 1 mM sodium pyruvate, were scraped and resuspended in PBS. Cells were plated at 2×10^4 cells/cm^2 in media containing 100 ng/ml of mouse RANKL (R&D Systems, Minneapolis, MN). Cells were allowed to differentiate for 3 (for immunofluorescence microscopy) or 4 days (for all other experiments). HOPs ($CD14^+$ peripheral blood mononuclear cells) were isolated from normal human peripheral blood mononuclear cells (AllCells, Emeryville, CA) using CD14 microbeads and MS columns (Miltenyi Biotec, Cologne, Germany) following the manufacturer's instructions. HOPs were plated at 3.1×10^5 cells/cm^2 in α-MEM (Invitrogen) containing 10% fetal calf serum (HyClone), 1 mM sodium pyruvate (HyClone), 25 ng/ml of human macrophage colony-stimulating factor, and 30 ng/ml of human RANKL (R&D Systems). Cells were allowed to differentiate for 7 or 10 days, with half of the media replaced every 3–4 days.

RT-PCR—RAW264.7 cells were treated with RANKL in 12-well plates as described above. After 1, 2, 3, and 4 days, total RNA was isolated. RNA was also prepared from control cells grown for 1 day in the absence of RANKL (non-differentiated). cDNA was prepared from 1 μg of RNA using ThermoScript reverse transcriptase and random hexamer primers (Invitrogen). PCR amplification using gene-specific primers was performed using HotStarTaq (Qiagen). Primer sequences were as follows (forward and reverse, respectively): Siglec-15, 5′-GCCCACGATCGCTATGAGAG-3′ and 5′-GGAAGCGGAACAGGTAGACG-3′, integrin β3, 5′-GCAAGCTTACTAGCAACCT-3′ and 5′-CATCAGACAGGACTCCCAC-3′, DC-STAMP, 5′-AGAGGAGAAGTCCTGGGAGTC-3′ and 5′-AAGGCAGAATCATGGACGAC-3′, Cathepsin K, 5′-TCTCTCGGCGTTTAATTTGG-3′ and 5′-TCTGCTGCACGTATTGGAAG-3′, tartrate-resistant acid phosphatase (TRAP), 5′-TTCCAGGAGACCTTTGAGGA-3′ and 5′-GTAGGCAGTGACCCCGTATG-3′, GAPDH, 5′-GTCAAGGCTGAGAACGGGAAG-3′ and 5′-GACGGCAGGTCAGGTCCAC-3′, NFATc1, 5′-CGAGATCACCTCCTACCTG-3′ and 5′-CCATTGAGACTGTACTTGCG-3′, and OSCAR, 5′-ACTCCTGGGATCAACGTGAC-3′ and 5′-GATAGCACATAGGGGGCAGA-3′.

Cell Stimulation—For cell stimulation with single antibodies, differentiation media was replaced with fresh growth media (without RANKL) containing the indicated antibody concentrations before lysing the cells at various times. For stimulations with primary and secondary (cross-linking) antibodies, differentiation media was replaced with cold growth media containing the primary antibody at 10 μg/ml, and cells were incubated 20 min at 4 °C. Media was then replaced with warm growth media containing goat anti-human IgG polyclonal antibody (Jackson ImmunoResearch, West Grove, PA) and cells were incubated for the indicated times at 37 °C before lysis.

Preparation of Cell Lysates and Immunoprecipitation—Cell lysates were prepared using mRIPA lysis buffer (50 mM Tris/HCl, pH 7.4, 1% Nonidet P-40, 0.25% deoxycholate, 150 mM NaCl) containing protease and phosphatase inhibitors (50 mM

NaF, 1 mM $NaVO_4$, and 1× Roche Complete EDTA-free phosphatase inhibitors). Lysate protein concentrations were measured by BCA assay (Pierce). For Western blotting of total cell lysates, equal amounts of protein (10–15 μg) were heat-denatured in SDS sample buffer containing β-mercaptoethanol, separated on a 10 or 12% SDS-PAGE gel, transferred to PVDF, and probed with the indicated antibodies. For immunoprecipitations, 2 (Fig. 6*A*) or 1 mg (Fig. 6*C*) of total lysates were incubated with 4 μg of antibody and 15 μl of Protein G-Sepharose beads for 4 h, rotating at 4 °C. After washing the beads 4 times with mRIPA, half of the precipitated material was analyzed by Western blotting, as above.

Immunofluorescence—For analysis of Siglec-15 localization in permeabilized cells (Fig. 1*B*), RAW264.7 cells or HOPs were differentiated, as described above, on glass coverslips (No. 1.5) or μ-Slide chambered coverslips (Ibidi) and fixed in 4% formaldehyde. Cells were permeabilized in 0.1% Triton X-100/PBS, blocked in 1.5% milk/PBS, and incubated with primary antibody (anti-Siglec-15 B02) at 2 μg/ml in blocking buffer followed by secondary antibody (donkey anti human-DyLight-488, Jackson ImmunoResearch) diluted 1:300 in blocking buffer. To stain nuclei, coverslips were incubated briefly in propidium iodide (10 μg/ml in PBS) prior to mounting using Prolong media (Invitrogen).

For characterization of Siglec-15 intracellular trafficking (Fig. 7*B*), RAW264.7-derived osteoclasts, grown on coverslips as above, were incubated with anti-Siglec-15 B02 or a control human IgG, diluted to 10 μg/ml in cold RAW264.7 growth media, for 20 min at 4 °C. After this "cold-loading" step, cells were either fixed immediately (as above), or incubated in fresh, warm media (without antibodies) for 10 or 45 min at 37 °C prior to fixation. Cells were blocked in PBS, 1% BSA, 0.1% saponin (PBS/BSA/Sap) + 2% goat serum and stained with anti-LAMP-2 diluted 1:20 in PBS/BSA/Sap followed by secondary antibodies (anti-human DyLight-488 and anti-rat rhodamine-X, Jackson ImmunoResearch), diluted 1:300 in PBS/BSA/Sap. Coverslips were mounted on glass slides using Prolong media.

Osteoclast TRAP Staining and Functional Assays—To test the effect of antibodies on osteoclast differentiation and function, cells were induced to differentiate, as described above, in media containing the indicated concentrations of antibodies. Osteoclasts were visualized after 4 days in culture by TRAP staining: briefly, cells were fixed in 3.7% formaldehyde, permeabilized with 0.2% Triton X-100/PBS, and incubated in TRAP staining buffer (100 mM sodium acetate, pH 5.2, 50 mM sodium tartrate, 0.01% Naphthol ASMX, and 0.06% Fast Red Violet) for ~30 min at 37 °C. The TRAP enzyme generates a red reaction product in osteoclasts. TRAP levels in osteoclast conditioned media were measured using the BoneTRAP ELISA kit (Immunodiagnostic Systems). To test osteoclast resorption activity, cells were seeded in wells coated with a calcium phosphate substrate (Osteologic, BD BioSciences) and induced to differentiate as above. After 7 days, wells were treated with bleach to remove cells, and areas of substrate resorption were observed by light microscopy.

Schenk Assay (BMD and MicroCT)—All animal procedures were carried out according to animal use protocols approved by the Animal Care Committee (ACC) of Mispro Biotech Services Inc. (Montreal, Quebec) in compliance with the guidelines of the Canadian Council on Animal Care (CCAC). Evaluation of *in vivo* efficacy was adapted from the methods described by Schenk and co-workers (18) using very young mice that have rapidly growing bones. Briefly, 3–4-week-old male mice (5 animals/group) were treated with PBS, a control mouse IgG, or the mouse B02 Siglec-15 antibody. The antibodies were administered intraperitoneally twice per week for 4 weeks using 26-gauge needles. The mice were sacrificed, blood was collected, and bones were dissected and fixed in 4% paraformaldehyde for 24 h. After washing in PBS, the bones were scanned using a PIXImus Densitometer (GE Medical Systems) to determine the bone mineral density (BMD) of the femurs, tibias, and vertebrae. Analyses of the bone microarchitecture and three-dimensional images of the bones were generated with a SkyScan high-resolution microCT (SkyScan Inc., Kontich, Belgium). Serum was prepared from blood samples and TRAP activity was measured using the MouseTRAP Assay ELISA kit (Immunodiagnostic Systems), following the manufacturer's instructions.

Bone Histomorphometry—Distal femurs were fixed in 4% paraformaldehyde for 48 h and washed in 1× PBS. Bone tissue was dehydrated in graded alcohols (70–100%), cleared in xylene, and embedded without decalcification in methyl methacrylate resin. Samples were cut into 5-μm sections and histochemically stained for TRAP and ALP activity. Three randomly selected regions of interest 500 μm below the growth plate within each distal femur were visualized using a Nikon Eclipse 90i microscope and a 10× objective. Image capture was performed using NIS Elements Imaging software (Nikon Inc., Melville, NY). Histomorphometric parameters were determined on the femoral secondary spongiosa at 10× using Adobe Photoshop and ImageJ software as described (19), following standard procedures published by the ASBMR Histomorphometry Nomenclature Committee (20).

Biotin Internalization Assay—To biotinylate cell-surface proteins, differentiated RAW264.7-derived osteoclasts were rinsed twice with cold PBS containing 1 mM $CaCl_2$ and 1 mM $MgCl_2$ (PBS/calcium/magnesium, HyClone) and incubated with the biotinylation reagent sulfo-NHS-SS-biotin (Pierce), diluted to 1 mg/ml in PBS/calcium/magnesium for 1 h at 4 °C. The reaction was stopped by quenching unreacted biotinylation reagent with glycine (100 mM in PBS/calcium/magnesium). To induce Siglec-15 internalization, cells were treated with anti-Siglec-15 B02 or a control human IgG alone or in combination with a secondary cross-linking antibody, as described under "Cell Stimulations." Following antibody treatments, cells were rinsed twice with cold NT buffer (20 mM Tris/HCl, pH 8.6, 150 mM NaCl, 1 mM EDTA, and 0.2% BSA) and incubated 2 × 25 min with sodium 2-mercaptoethane sulfonate (MesNa), prepared at 25 mM in cold NT buffer, to reduce the disulfide bond of sulfo-NHS-SS-biotin and thereby remove any remaining cell-surface biotin. To gauge the maximum possible level of Siglec-15 biotinylation, this MesNa treatment was omitted for one control (these control cells were incubated 2 × 25 min with NT buffer alone). The remaining MesNa was then

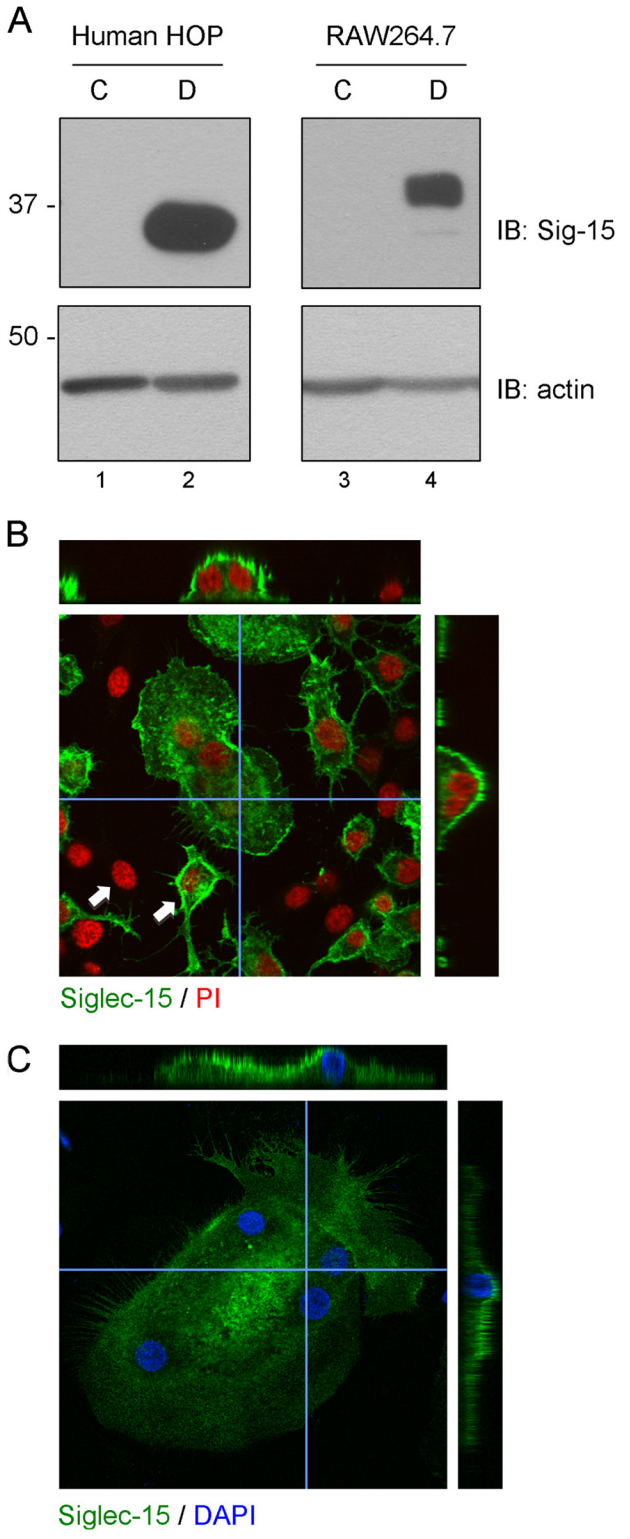

FIGURE 1. **Expression and localization of Siglec-15 protein in osteoclasts.** *A,* Western blots of total protein extracts from human HOP- and mouse RAW264.7-derived osteoclasts (*D*) and non-differentiated precursor cells (*C*). *B* and *C,* confocal microscopy analysis of Siglec-15 localization in RAW264.7- and HOP-derived osteoclasts. *B,* RAW264.7 cells were grown for 3 days on glass coverslips in the presence of RANKL. Fixed and permeablized cells were then stained with anti-Siglec-15 and propidium iodide (*PI*). *Z*-stacks were prepared by acquiring confocal images at 1-μm intervals throughout the depth of the cells in the field. The *central panel* shows a single confocal image of a multinucleated osteoclast surrounded by non-fused precursor cells. The *two arrows* indicate examples of mononuclear cells that are positive or negative for Siglec-15 expression. The *narrow panels on top* and *right* are cross-sections through the osteoclast generated by re-slicing a three-dimensional reconstruction prepared from the image stack (the slices were performed along the paths indicated by the *blue horizontal* and *vertical lines*). *C,* human HOP-derived osteoclasts were grown on chamber slides, fixed, and stained with anti-Siglec-15 and DAPI. Analysis by confocal microscopy was performed as described in *B*.

quenched with iodoacetamide, diluted to 5 mg/ml in PBS/calcium/magnesium, for 15 min.

To evaluate the amount of biotinylated Siglec-15 that had been internalized by the osteoclasts, cells were lysed in mRIPA, as described above. Biotinylated proteins were collected by streptavidin pull-down: 250 μg of lysate was incubated overnight with 50 μl of Dynal MyOne streptavidin beads (Invitrogen), rotating at 4 °C. After extensive washing, Siglec-15 was detected in the precipitated material by Western blotting.

Fab Preparation and Analysis—Fab fragments were obtained from antibody B02 by ficin digest using the Mouse IgG1 Fab and $F(ab')_2$ Preparation Kit (Pierce), according the manufacturer's instructions.

The ability of the B02 Fab to bind Siglec-15 on the cell surface was evaluated by FACS. 293-6E cells were transfected with pCDNA3.1-hSiglec-15; this plasmid consists of the full-length human Siglec-15 cDNA cloned between the HindIII and XhoI sites of pCDNA3.1-myc-his-A (a stop codon prevents expression of the myc-His tag). At 24 h post-transfection, 200 μl of the indicated concentrations of antibody/Fab, diluted in FCM buffer (PBS, 0.5% BSA), were added to 200,000 cells, resuspended in 50 μl of the same buffer. After a 1-h incubation (on ice) and washing with PBS, 200 μl of secondary antibody (FITC-conjugated anti-mouse κ light chain-specific polyclonal antibody, Southern Biotech), diluted 1:200 in FCM buffer, was added for 1 h. After an additional washing, cells were suspended in ~300 μl of FCM buffer, and 4 μl of propidium iodide, diluted to 1 mg/ml in PBS, was added just before analyzing cells with a flow cytometer (FACScan, BD Biosciences). Non-viable cells that stained positive with propidium iodide were excluded from analysis.

RESULTS

Expression and Localization of Siglec-15 Protein during Osteoclastogenesis—Individual clones from a library of monoclonal antibodies generated against the extracellular region of Siglec-15 were evaluated in detail for their performance in various applications. Although for potential therapeutic candidates we selected antibodies that bound the native form of Siglec-15 and had activity on intact cells, we also identified distinct clones that were particularly effective for immunoprecipitation and Western blotting. These reagents have allowed us to elaborate on our previous studies to examine Siglec-15 expression and subcellular localization. We prepared protein lysates from HOP- and RAW264.7-derived osteoclasts as well as from corresponding non-differentiated control cells. As shown in Fig. 1*A*, by Western blotting, there was a dramatic increase in Siglec-15 protein in both the human and murine differentiated osteoclasts (see Fig. 1*A*, *lanes 2* and *4*), in agreement with previous RT-PCR experiments (3, 5).

We also analyzed Siglec-15 expression in differentiated osteoclasts by confocal microscopy. As shown in Fig. 1, *B* and *C,* for

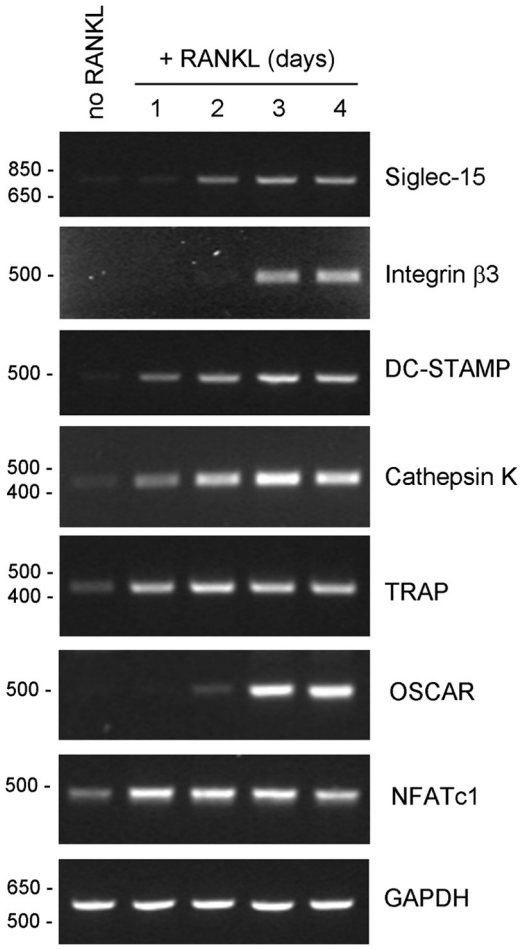

FIGURE 2. **Siglec-15 mRNA is induced with intermediate kinetics relative to other genes up-regulated during osteoclast differentiation.** RT-PCR was performed on RNA isolated from RAW264.7 cells, either untreated (no RANKL) or treated with RANKL for 1, 2, 3, or 4 days.

RAW264.7 and HOP cultures, strong Siglec-15 immunofluorescence is observed in multinucleated osteoclasts, and it is evident from cross-sectional slices that Siglec-15 is predominantly localized at the cell surface.

RAW264.7 cultures treated for 3 days with RANKL consist of both small (5–10 nuclei) osteoclasts and non-fused precursor cells. Interestingly, all of the multinuclear osteoclasts in these cultures stained strongly for Siglec-15, whereas some, but not all, of the mononuclear cells also expressed the protein (see *white arrowheads* in Fig. 1*B*). In cultures of untreated RAW264.7 cells, no cells stained for Siglec-15 (data not shown).

To investigate further the kinetics of Siglec-15 expression during osteoclastogenesis, we performed RT-PCR analysis of gene expression in RAW264.7 cells treated for 1–4 days with RANKL. RAW264.7 exposed to RANKL begin to fuse to form osteoclast-like cells after 3 days. As shown in Fig. 2, increased Siglec-15 mRNA is observed prior to cell fusion, at day 2; Siglec-15 is induced with kinetics similar to the osteoclast collagen receptor OSCAR. In comparison, the critical osteoclast transcription factor NFATc1, as well as cathepsin K, TRAP, and DC-STAMP are clearly induced earlier than Siglec-15. Notably, DC-STAMP is an important mediator of osteoclast fusion (21), although its expression is induced after 1 day, well before fusion occurs. In contrast, induction of β3 integrin, which is expressed specifically in multinucleated osteoclasts (22), occurs later than Siglec-15, at day 3. These gene expression results demonstrate that Siglec-15 is not among the genes initially induced by RANKL stimulation and that its expression likely precedes osteoclast precursor fusion, in agreement with our immunofluorescence data.

Siglec-15 Monoclonal Antibodies Inhibit Osteoclast Formation in Vitro and in Vivo—A primary criterion for selecting specific Siglec-15 antibodies as potential therapeutics for bone loss was their ability to inhibit osteoclast differentiation *in vitro*. Our *in vitro* assay system consisted of HOPs, which readily differentiate into TRAP positive multinuclear osteoclasts when treated for 7 days with macrophage colony-stimulating factor and RANKL. To assess osteoclast activity, HOPs were differentiated on a bone-like mineralized matrix, which functional osteoclasts are able to digest. We identified several monoclonal antibodies that were effective in this assay, but as shown in Fig. 3*A*, clone E09 was particularly promising. Under control conditions, HOPs differentiated into large, well spread, TRAP-positive osteoclasts in a RANKL-dependent manner; these osteoclasts actively digested a mineralized calcium phosphate substrate. In the presence of antibody E09, some TRAP-positive cells still formed, but few had more than one nucleus and their morphology was clearly altered (Fig. 3*A*, *top right panel*). Furthermore, their capacity to digest the mineralized substrate was greatly reduced (Fig. 3*A*, *lower right panel*). Notably, as shown in Fig. 3*B*, when HOPs are allowed to differentiate in the presence of E09 beyond 7 days, they eventually fuse, although their altered morphology relative to normal osteoclasts is still evident. The multinucleated cells formed in the presence of E09 display intense intracellular TRAP staining, but secretion of this enzyme into the culture media is greatly reduced (Fig. 3*C*).

Another antibody, designated B02, was selected for its ability to bind to the murine form of Siglec-15 and was tested in the RAW264.7 osteoclast differentiation model. RAW264.7 cells treated with RANKL in the presence of B02 became TRAP-positive but largely failed to fuse (Fig. 3*D*). Together, these results are in agreement with our findings on the inhibitory effects of Siglec-15 RNAi on osteoclastogenesis in RAW264.7 and primary human cells (3).

To test the physiological importance of Siglec-15 and validate our cell-based results, we tested the monoclonal anti-Siglec-15 antibodies *in vivo*. For these experiments, we treated 4-week-old mice with the B02 antibody for 4 weeks and assessed the effects of this treatment on the long bones and the vertebrae. Because mice have rapidly growing bones at this age, the perturbation of osteoclast activity by anti-resorptives can provoke a rapid, dramatic increase in BMD in a relatively short period of time. Following the treatment period, the animals were euthanized, the bones were dissected and scanned by densitometry to determine the BMD. As shown in Fig. 4*A*, compared with a control mouse IgG (IgG (10)), treatment with the anti-Siglec-15 monoclonal antibody resulted in a considerable, dose-dependent increase in BMD in the right femur (Fig. 4*A*, *left panel*), right tibia (Fig. 4*A*, *middle panel*), and vertebra (Fig. 4*A*, *right panel*) of these mice. To further examine the changes in BMD, selected bone samples were scanned using x-ray

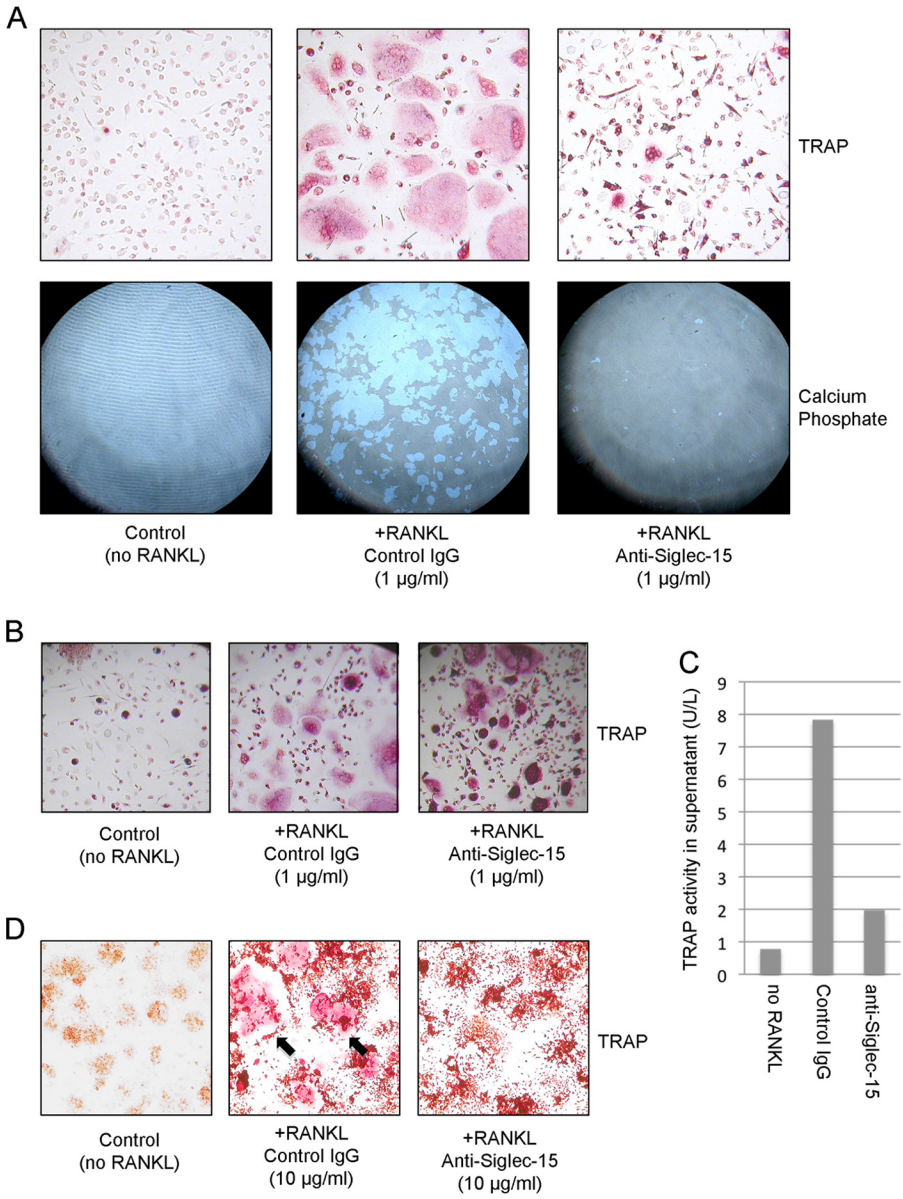

FIGURE 3. **Siglec-15 antibodies inhibit osteoclast differentiation and activity *in vitro*.** *A,* HOPs were grown with macrophage colony-stimulating factor alone (*left panels*) or with macrophage colony-stimulating factor and RANKL (to induce osteoclast differentiation) in the presence of control human IgG (*middle panels*) or anti-Siglec-15 (*right panels*) for 7 days. Cells were grown in parallel either on plastic (*top panels*) or on calcium phosphate-coated (*bottom panels*) plates. Multinucleated osteoclasts were identified on plastic by TRAP staining (*red*). Regions of calcium phosphate resorption were visualized by phase-contrast mode light microscopy after cell removal. *B,* upon prolonged treatment with RANKL (10 days rather than 7 days), HOPs grown in the presence of anti-Siglec-15 E09 fuse to form intensely TRAP-stained, multinucleated cells (*right panel*). The morphology of these cells is distinct from normal osteoclasts formed in the presence of a control antibody (*middle panel*). *C,* HOPs differentiated with RANKL in the presence of anti-Siglec-15 E09 display impaired TRAP secretion. TRAP levels in conditioned media of HOPs differentiated for 10 days were determined by ELISA. *D,* Siglec-15 antibody B02 inhibits differentiation of mouse RAW264.7 cells into osteoclasts. RAW264.7 cells were treated with RANKL to induce differentiation in the presence of control human IgG (*middle panel*) or anti-Siglec-15 B02 (*right panel*). Control cells were grown without RANKL or antibodies (*left panel*). After 3 days in culture, cells were stained for TRAP activity (*red*). The *black arrows* in the *middle panel* indicate examples of multinuclear, TRAP-positive osteoclasts.

microtomography (MicroCT) to analyze their microarchitecture. In agreement with the densitometry results, we observed a marked increase in trabecular volume in the femurs and the vertebra of mice treated with the anti-Siglec-15 antibody compared with the control IgG-treated mice (see the representative cross-sectional views of the right femur (*upper panels*) and the L5 vertebra (*lower panels*) in Fig. 4*B*). In agreement with these qualitative observations, quantitative measurements of the microCT scans (Table 1) confirmed the increase in bone mineral density in the animals treated with the Siglec-15 antibody. In particular, there were statistically significant increases in bone volume, bone surface, trabecular number, and connectivity density. Conversely, the trabecular separation was significantly decreased, a change that was in line with the increased density of trabecular structures. Overall, the increase in trabecular bone volume (BV/TV) exceeded 55% compared with the vehicle-treated animals. To provide additional confirmation that these changes in bone structure were due to effects on osteoclasts, we analyzed TRAP levels in the serum of these mice by ELISA at the conclusion of the study. As shown in Fig. 4*C*,

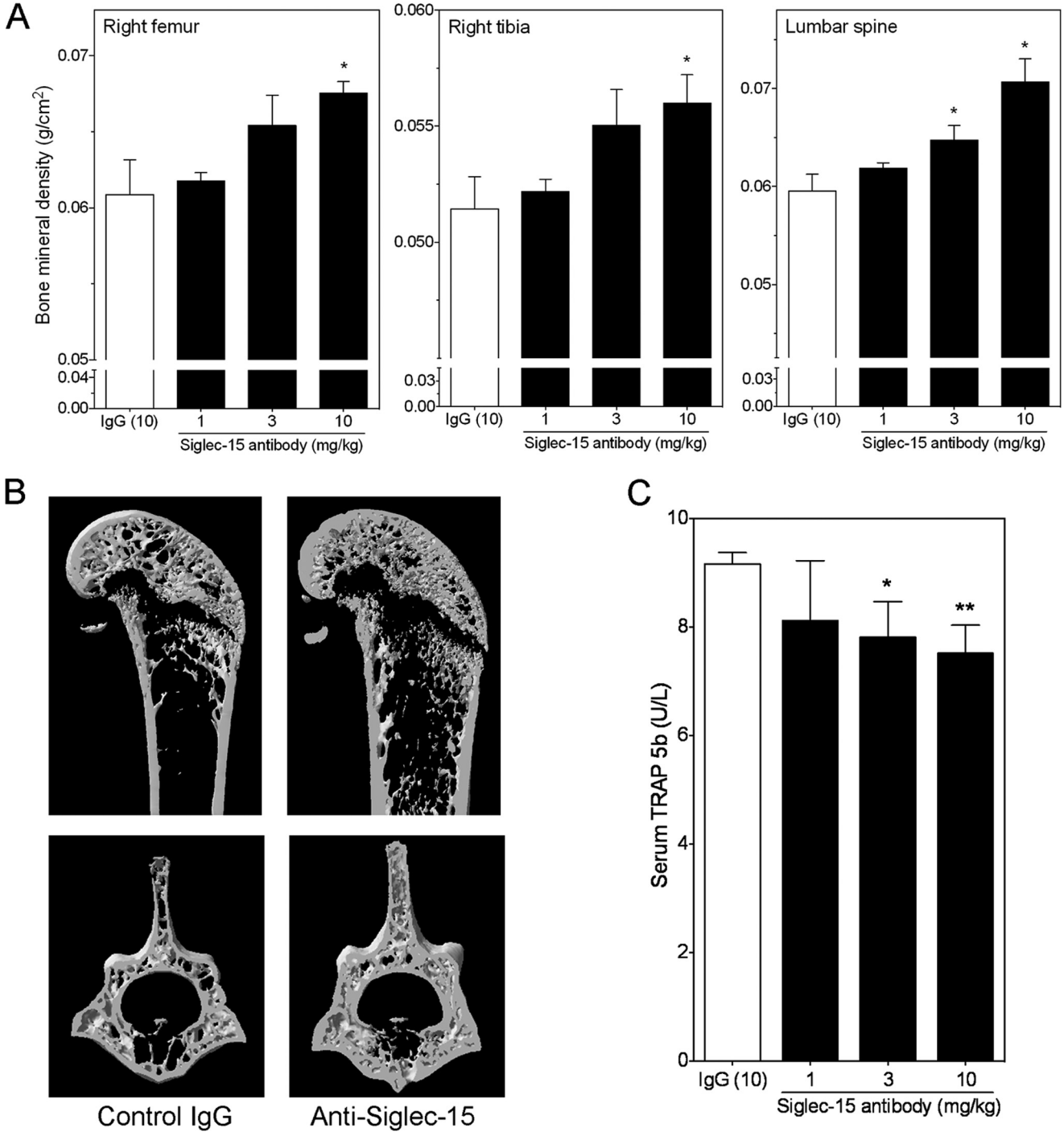

FIGURE 4. **Treatment with Siglec-15 antibodies increases bone mineral density in mice.** Three- to 4-week-old male mice were treated with the B02 Siglec-15 antibody twice per week at 1, 3, or 10 mg/kg for 4 weeks. *A,* bone mineral density of long bones (*left panel*, right femur; *middle panel*, right tibia) and the lumbar vertebrae (L4–L6, *right panel*) were measured with a densitometer. The control group was treated similarly with a murine IgG at 10 mg/kg. *B,* cross-sectional images of a representative right femur (*top panels*) dissected from a control IgG-treated mouse (control IgG, *left panel*) or a mouse treated with 10 mg/kg of the B02 Siglec-15 antibody (Anti-Siglec-15, *right panel*). Similar cross-sectional images of the L5 vertebra from the same mice are shown in the *lower panels*. *C,* osteoclast-specific TRAP (TRAP 5b) activity was measured by ELISA in serum prepared from a terminal bleed. *p* values (*versus* the IgG treated group, $n = 5$/group) were calculated using Student's *t* test. *, $p < 0.05$; **, $p < 0.02$.

there was a significant decrease in osteoclast-specific TRAP 5b (TRAP) activity in the 3 and 10 mg/kg dose groups. Interestingly, histological examination of bone sections from these mice showed that both osteoclast (Fig. 5, *A* and *B*) and osteoblast (Fig. 5, *C* and *D*) numbers (relative to trabecular bone surface) were increased in the Siglec-15 antibody-treated animals. These *in vivo* results are consistent with the observed effects of Siglec-15 antibodies on osteoclast differentiation *in vitro*. In particular, the antibodies delay fusion of osteoclast precursors *in vitro*, but some TRAP-positive multinucleated cells still eventually form. If the same effect occurs *in vivo*, the multinucleated cells formed in the presence of Siglec-15 anti-

TABLE 1

MicroCT assessment of trabecular bone architecture of the right femur of mice treated with Siglec-15 antibody

The data represent the mean ± S.E. ($n = 5$). The abbreviations used are: BV/TV, percent bone volume; Tb.No, trabecular number; Tb.Th, trabecular thickness; Tb.Sp, trabecular separation; BS/TV, bone surface density; Conn.Dn, connectivity density.

	Control IgG	Siglec-15 mAb
BV/TV (%)	6.4 ± 0.60	10 ± 1.8[a]
Tb.No (1/mm)	1.23 ± 0.103	2.01 ± 0.336[a]
Tb.Th (mm)	0.052 ± 0.0015	0.049 ± 0.0008
Tb.Sp (mm)	0.283 ± 0.0140	0.206 ± 0.0236[a]
BS/TV (1/mm)	6.97 ± 0.566	11.1 ± 1.50[a]
Conn.Dn (1/mm^3)	501 ± 71.5	996 ± 186[a]

[a] *p* value control IgG *versus* Siglec-15 mAb <0.05.

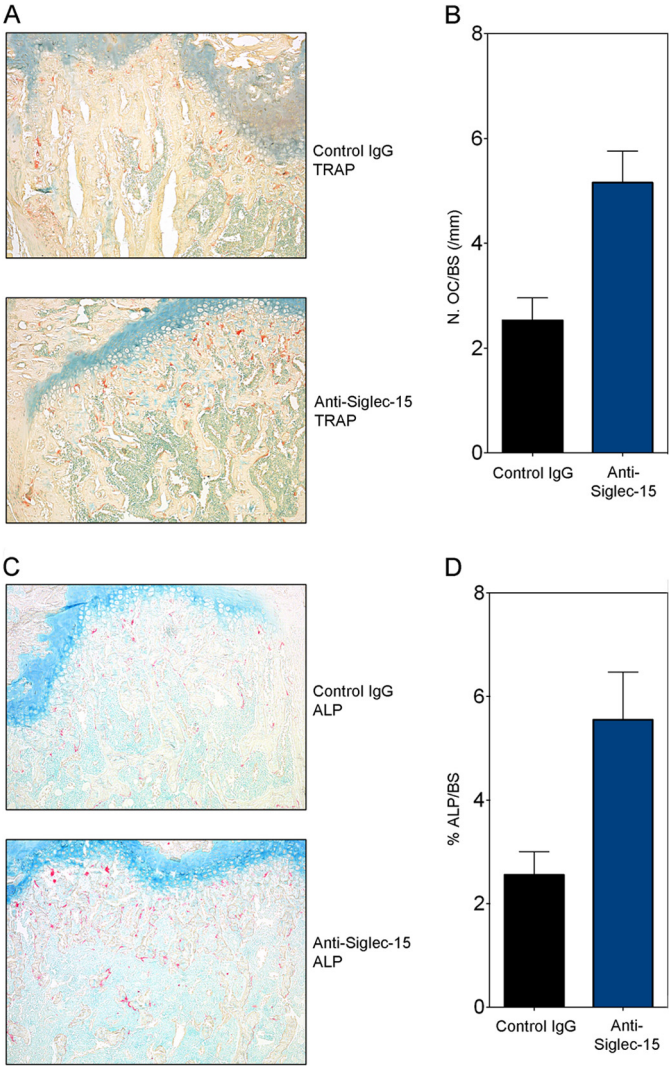

FIGURE 5. **Treatment with Siglec-15 antibody results in increased osteoclast number and osteoblast surface.** *A*, representative photomicrographs (×10 magnification) of undecalcified mouse femur sections treated with control antibody (IgG) or anti-Siglec-15, histochemically stained with TRAP (*A*) and ALP (*C*). *Scale bar*, 100 μm. Histomorphometrical analysis was performed. *B*, N.Oc/BS, number of TRAP-positive osteoclasts per trabecular bone surface (mm). *D*, Ob.S/BS, ALP-positive osteoblast-surface per bone surface. *p* values (*versus* the IgG treated group, $n = 5$/group) were calculated using the Student's *t* test. *, $p < 0.05$.

bodies would still be counted as osteoclasts upon histological examination of bone sections.

Siglec-15 Associates with DAP12 in Osteoclasts and Antibody-induced Clustering Induces Akt and DAP12 Phosphorylation—Although our results established that Siglec-15 is required for formation of functional osteoclasts, the underlying molecular mechanisms remained to be determined. An important clue came from the presence of a lysine residue in the Siglec-15 transmembrane domain (Lys-273), suggesting an interaction with the transmembrane adapter protein DAP12. Indeed, a recent study demonstrated that upon co-overexpression of epitope-tagged forms of Siglec-15 and DAP12 in 293T cells, a complex could be detected, which was dependent on the presence of Lys-273 (14). We were also able to detect this complex under similar overexpression conditions (data not shown), and we proceeded to determine whether the complex is also present at endogenous expression levels in osteoclasts. Protein lysates were prepared from differentiated RAW264.7-derived osteoclasts as well as from non-differentiated control cells, and immunoprecipitations were performed using Siglec-15 and DAP12 antibodies. As shown in Fig. 6*A*, DAP12 was readily detected in protein complexes precipitated with anti-Siglec-15, and likewise, anti-DAP12 precipitated abundant Siglec-15. As expected, based on Siglec-15 protein expression levels, this complex was highly osteoclast-specific and was not detected in non-differentiated cells. Notably, DAP12 expression was not dramatically altered during RAW264.7 osteoclast differentiation. Another DAP12-associated immunoglobulin-like receptor, TREM-2, is expressed in osteoclasts and is important for their differentiation and activity (23). We were able to detect a TREM-2·DAP12 complex that was present at similar levels in control and differentiated RAW264.7 cells (data not shown), indicating that the abundant Siglec-15·DAP12 complexes present in osteoclasts do not reduce TREM-2·DAP12 binding.

Previous studies showed that when phosphorylated on its ITAM motif, DAP12 is capable of activating a number of signaling pathways, including PI3K-Akt, PLCγ, and Grb2-Ras-Erk cascades (12). However, the signaling output of DAP12 in specific contexts is highly dependent on its associated receptor (12). In the absence of an identified natural ligand or molecular partner for Siglec-15, we used an antibody cross-linking approach to evaluate the ability of Siglec-15 to activate intracellular signaling. Initially, we treated RAW-derived osteoclasts with anti-Siglec-15 for multiple time points up to 30 min but failed to observe any activation of Akt, PLCγ, or ERK (data not shown). However, for several other DAP12-associated receptors, higher-order clustering of the receptor, rather than bivalent antibody-induced dimerization, is required to induce ITAM-dependent signaling (12, 24). To induce multimerization, we treated cells with a primary Siglec-15 antibody followed by a secondary, cross-linking antibody. Under these conditions, we observed a signaling effect (Fig. 6*B*, *lanes 5*, *8*, and *11*), with Akt becoming strongly phosphorylated within minutes of secondary antibody cross-linking. Maximum phosphorylation of Akt was achieved after 5 min of treatment with anti-Siglec-15 (Fig. 6*B*, *lane 8*). In contrast, phospho-ERK (Fig. 6*B*) and phospho-PLCγ (not shown) were not modulated. Consistent with the lack of expression of Siglec-15, there was no activation of Akt in non-differentiated RAW264.7 cells under the same conditions (Fig. 6*B*, see *lanes 1*, *4*, *7*, and *10*). Similarly, substitution of the primary Siglec-15 antibody with a control

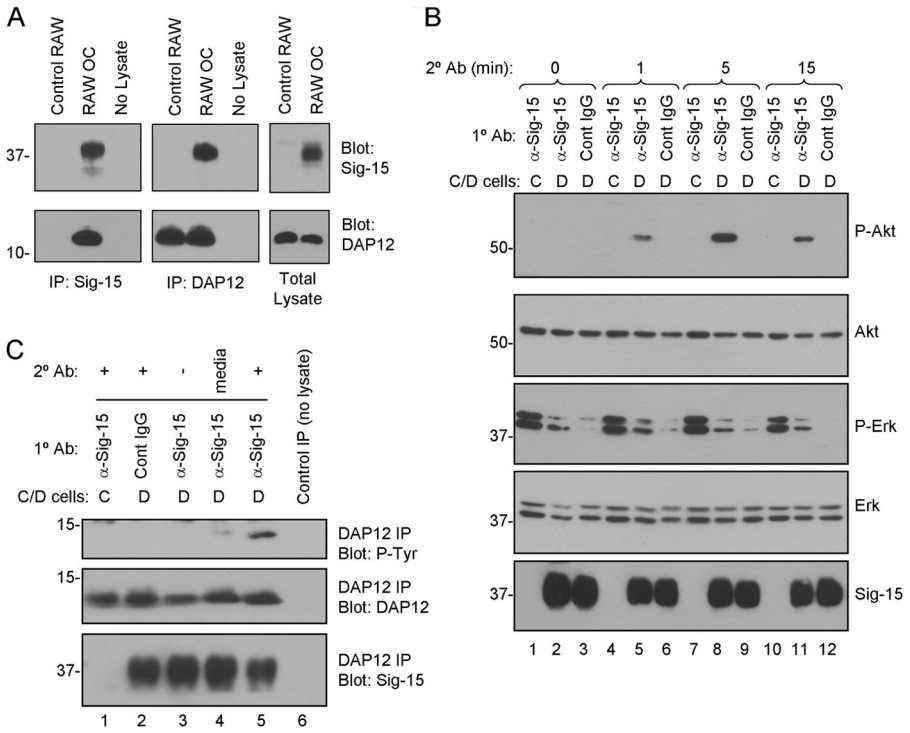

FIGURE 6. **Siglec-15 and DAP12 form a complex in osteoclasts, and Siglec-15 clustering induces DAP12 phosphorylation and Akt signaling.** *A,* co-immunoprecipitation (*Co-IP*) of DAP12 and Siglec-15. Protein lysates were prepared from non-differentiated RAW264.7 cells (control RAW) or RAW264.7-derived osteoclasts. Siglec-15 (*left panels*) and DAP12 (*middle panels*) immunoprecipitates as well as total lysates (*right panels*) were analyzed by Western blotting with Siglec-15 and DAP12 antibodies. The *no lysate* IPs were performed using fresh lysis buffer. *B*, analysis of cell signaling induced by Siglec-15 clustering. Control (*C*) or differentiated (*D*) RAW264.7 cells were treated with primary antibody (anti-Siglec-15 or control human IgG) at 4 °C followed by a secondary cross-linking antibody for the indicated times at 37 °C. Total lysates were analyzed by Western blotting with the indicated antibodies. *C,* DAP12 phosphorylation following Siglec-15 cross-linking. RAW264.7 cells were treated as in *B* for 5 min with secondary antibody (*lanes 1*, *2*, and *5*). As additional controls, some cells were lysed immediately after primary antibody incubation (*lane 3*) and for others, the secondary antibody was omitted from the 37 °C incubation media (*lane 4*). Protein extracts were prepared, and DAP12 immunoprecipitates were analyzed by blotting with anti-phosphotyrosine, anti-DAP12, and anti-Siglec-15 antibodies.

human IgG eliminated the signaling response (Fig. 6*B*, see *lanes 3*, *6*, *9,* and *12*). These results demonstrated that Siglec-15 cross-linking specifically activates Akt without affecting ERK or PLCγ, two other pathways commonly downstream of DAP12 (12, 24).

If induction of cell signaling by Siglec-15 is dependent on the DAP12 ITAM motif, tyrosine phosphorylation of DAP12 should be detectable upon Siglec-15 clustering. To test this, we immunoprecipitated DAP12 and evaluated its phosphorylation by Western blotting (Fig. 6*C*). In RAW264.7-derived osteoclasts stimulated with primary/secondary antibodies to cross-link Siglec-15 (as described above), we detected tyrosine-phosphorylated DAP12 at 12 kDa (Fig. 6*C*, *lane 5*). In non-differentiated cells treated in the same manner or osteoclasts treated with a control human IgG, little or no DAP12 phosphorylation was detected. Notably, although abundant Siglec-15 was co-precipitated with DAP12 from the differentiated osteoclasts (as expected), no phosphotyrosine signal was detected at its molecular mass (37 kDa), indicating that phosphorylation of the cytoplasmic tyrosine residue of Siglec-15, part of its putative ITAM, is not involved in the signaling response (data not shown). Thus, our results are consistent with DAP12 acting as a signaling module for Siglec-15; DAP12 becomes phosphorylated following Siglec-15 clustering, likely leading to recruitment of signaling molecules to its ITAM motif and activation of the Akt pathway.

Siglec-15 Is Internalized and Degraded following Antibody Ligation—The ability to mediate endocytosis of bound ligands and antibodies is a common feature of several members of the Siglec family; indeed, the cellular uptake of therapeutic antibodies is a critical aspect of the mechanism of action of antibody-drug conjugates targeting the CD22 and CD33 Siglecs (4). Interestingly, Siglec-15 also contains a *YXXΦ* sequence in its cytoplasmic domain (this tyrosine, Tyr-309, is also part of the putative ITAM, discussed above); YXXΦ motifs can interact with the clathrin adapter AP-2 to regulate receptor internalization (14, 25). Thus, we investigated the effect of antibody ligation on Siglec-15 endocytosis in osteoclasts.

We first tested whether a Siglec-15 antibody, either alone or in combination with a secondary cross-linking antibody, could induce internalization of Siglec-15, labeled with biotin, from the surface of RAW264.7-derived osteoclasts. After the antibody stimulation, any remaining cell-surface biotin was released by treatment with a reducing agent. Cells were then lysed, and internalized biotinylated proteins were collected with streptavidin beads. Siglec-15 was detected in the precipitated material by Western blotting. Interestingly, we found that treatment with Siglec-15 antibody alone induced substantial internalization compared with a control human IgG (Fig. 7*A*, compare *lanes 7* and *8*), whereas addition of a secondary antibody to induce receptor clustering, which is required for acti-

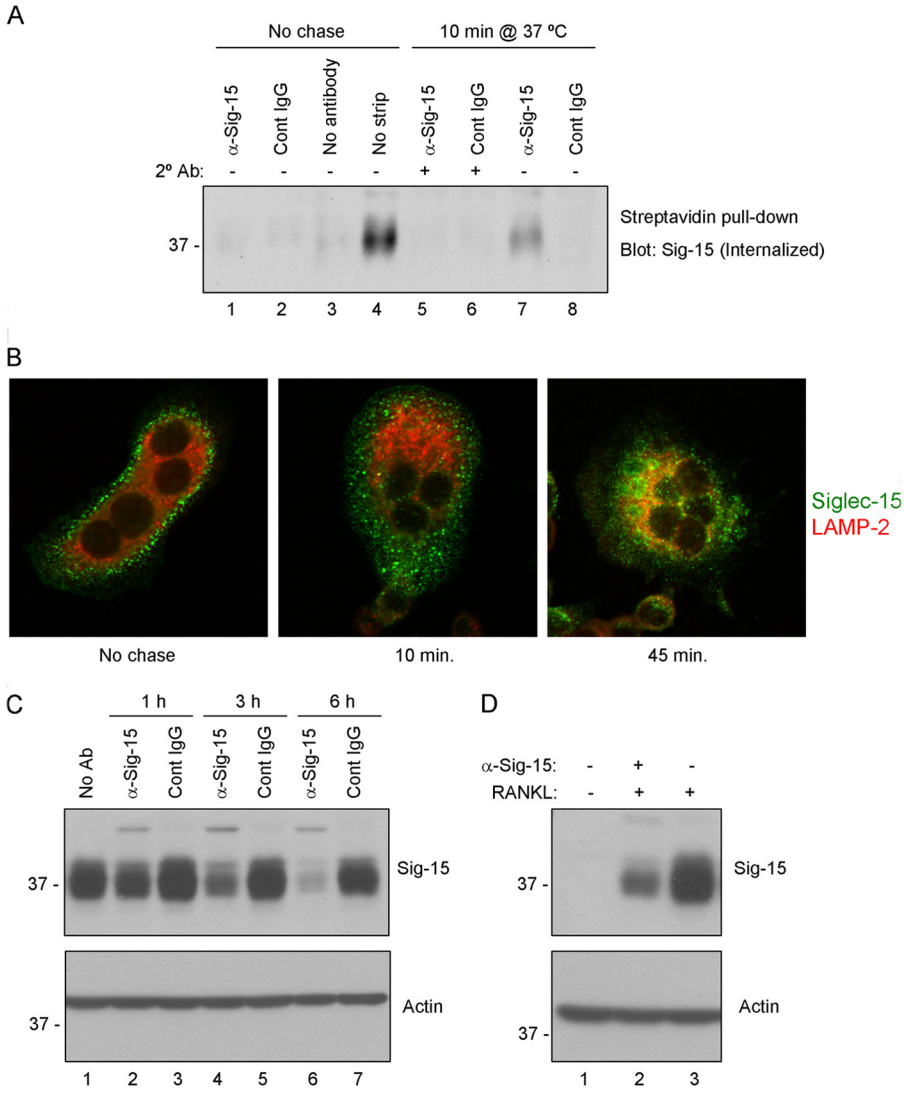

FIGURE 7. **Antibody-induced internalization and lysosomal degradation of Siglec-15 in osteoclasts.** *A,* internalization of biotinylated Siglec-15. RAW264.7-derived osteoclast cell-surface proteins were labeled with a disulfide-linked biotinylation reagent. Cells were then treated with a combination of primary (anti-Siglec-15 B02 or control IgG) antibodies (at 4 °C) followed by secondary cross-linking antibodies (10 min at 37 °C, *lanes 5* and *6*), or with primary antibody alone (10 min at 37 °C, *lanes 7* and *8*). Control cells were incubated with B02, control IgG, or no antibody at 4 °C (*lanes 1–3*) without a 37 °C chase. After these antibody treatments, remaining cell-surface biotin was stripped with a reducing agent; for one sample, as an additional control (*lane 4*), this stripping step was omitted. Internalized, biotinylated proteins were collected from cell lysates by streptavidin immunoprecipitation, and Siglec-15 was detected by Western blotting. *B,* characterization of Siglec-15 endocytosis by confocal microscopy. RAW264.7-derived osteoclasts were cold-loaded with Siglec-15 antibody and either fixed immediately (*No chase*) or incubated in fresh, warm media for 10 or 45 min prior to fixation. Cells were then permeablized and stained with anti-LAMP2 and anti-human IgG (to detect internalized Siglec-15). *C,* Siglec-15 protein levels decrease rapidly following antibody treatment. Differentiated RAW264.7-derived osteoclasts were treated for the indicated times with anti-Siglec-15 or a control human IgG. Protein lysates were analyzed by Western blotting with the indicated antibodies. *D,* RAW264.7 differentiated in the presence of Siglec-15 antibodies show decreased Siglec-15 protein levels. Protein lysates of RAW264.7 cells, either non-differentiated (− *RANKL*) or differentiated (+ *RANKL*) in media with or without anti-Siglec-15 were analyzed by Western blotting with the indicated antibodies.

vation of Akt signaling, had less of an effect than the single antibody (Fig. 7*A*, *lane 5*).

We proceeded to characterize the antibody-induced endocytosis of Siglec-15 by immunofluorescence microscopy. RAW264.7-derived osteoclasts, growing on glass coverslips, were cold-loaded with anti-Siglec-15 diluted in normal growth media at 4 °C, conditions that should permit antibody binding but not endocytosis. Cells were then fixed immediately or incubated in antibody-free warm media for different times prior to fixation. As expected based on the distribution of Siglec-15 in fixed, permeabilized osteoclasts (Fig. 1*B*), in intact osteoclasts, cold-loaded Siglec-15 antibodies bound strongly at the cell surface (Fig. 7*B*, *left panel*). After a 10-min incubation at 37 °C, the staining pattern was clearly altered: Siglec-15 antibodies were present in internal punctae that are likely endosomes (Fig. 7*B*, *center panel*). This rapid internalization is in excellent agreement with our biotinylation assay results described above (Fig. 7*A*). Although after 10 min the Siglec-15 signal was still near the plasma membrane, after 45 min it became mostly perinuclear (Fig. 7*B*, *right panel*), which is a typical lysosomal staining pattern (26). This was confirmed by co-staining these cells for the lysosome marker LAMP-2. Indeed, at 45 min there was substantial co-localization of Siglec-15 and LAMP-2 in perinuclear regions, whereas at earlier time points, the staining patterns were clearly divergent (Fig. 7*B*).

Lysosomes are principal sites of receptor degradation following endocytosis. To determine whether this is the fate of Siglec-15, we treated RAW264.7-derived osteoclasts with antibodies over a prolonged time course and analyzed total protein extracts by Western blotting. As shown in Fig. 7*C*, there was a clear decrease in Siglec-15 protein levels beginning within 3 h of addition of anti-Siglec-15 (*lanes 4* and *6*). In contrast, exposure of the osteoclasts with a control IgG did not cause this reduction in signal (Fig. 7*C*, *lanes 5* and *7*). Notably, a similar reduction in Siglec-15 protein levels was detected in RAW264.7 cells differentiated with RANKL (for 4 days) in the presence of anti-Siglec-15 (Fig. 7*D*). Together, these results demonstrated that bivalent anti-Siglec-15 antibodies induce rapid internalization of the receptor, which is then targeted to lysosomes for degradation.

Monovalent Anti-Siglec-15 B02 Fab Has Reduced Ability to Induce Siglec-15 Degradation and Inhibit Osteoclast Differentiation—To evaluate receptor degradation as a potential mechanism of action of our monoclonal antibodies, we compared the activities of anti-Siglec-15 IgG to a corresponding Fab fragment. Fabs are monovalent and should not induce dimerization, which we suspected might be required for receptor down-regulation induced by the intact IgG. Fab fragments were generated from antibody B02 by ficin digestion. By ELISA, we found that the monovalent fragments retained an ability to bind Siglec-15 that was very similar to the full IgG (data not shown). Similarly, like the intact antibody, the Fab was able to bind Siglec-15 on the surface of transfected cells as detected by flow cytometry (Fig. 8*A*). In contrast, when applied to RAW264.7-derived osteoclasts, the B02 Fab induced degradation of Siglec-15 to a lesser extent than the full IgG (Fig. 8*B*). Furthermore, the ability of the B02 Fab to inhibit osteoclast differentiation was reduced relative to the full antibody (Fig. 8*C*). These results provided a functional link between the effect of Siglec-15 antibodies on osteoclastogenesis and their ability to induce receptor dimerization and endocytic down-regulation.

DISCUSSION

In this article, we confirm the functional importance of Siglec-15 in the differentiation and activity of osteoclasts, and we address the molecular mechanism underlying the inhibitory activity of monoclonal antibodies against this protein. Our results suggest that the specificity of Siglec-15 expression could make it an ideal target in terms of avoiding non-osteoclast-associated secondary effects of current therapeutics. Although Siglec-15 protein is highly up-regulated during osteoclast differentiation both in RAW264.7 and primary human cells as demonstrated by Western blotting and immunofluorescence, the protein is undetectable in non-differentiated cells. Similarly, by flow cytometry, we were unable to detect any substantial Siglec-15-positive population of circulating hematopoietic cells in mouse bone marrow, spleen, or peripheral blood.[3] This is consistent with our earlier findings showing that Siglec-15 mRNA, with the exception of weak expression in lung, is absent from an extensive panel of normal human tissues (3).

In cultured osteoclast precursors, treatment with monoclonal antibodies against Siglec-15 inhibited formation of mature osteoclasts capable of resorbing mineralized substrate. Notably, HOPs induced to differentiate in the presence of anti-Siglec-15 still became TRAP-positive and eventually fused to form multinucleated cells, although their morphology was greatly altered relative to normal human osteoclasts. These results indicate that Siglec-15 antibodies affect osteoclast differentiation at a late stage.

Very recently, following completion of the current study, two groups have independently generated full-body *siglec-15*$^{-/-}$ mice (27, 28). These mice are viable and healthy and display a mildly osteopetrotic phenotype. Notably, one of these groups found no significant change in osteoclast numbers in the null mice, whereas the other reported a modest decrease in the same parameter. In our *in vivo* experiments, we found that treatment of young mice for a short period of time with Siglec-15 antibodies led to a significant increase in osteoclast numbers. Several studies have found that other treatments that affect osteoclast activity lead to an accumulation of non-resorbing osteoclasts in bone (29). Based on the effects of Siglec-15 antibodies on osteoclast differentiation *in vitro* and on BMD and serum TRAP levels *in vivo*, we strongly suspect that the osteoclasts present in the treated mice have reduced activity.

Because of the importance of osteoclast-derived factors in promoting osteoblast-dependent bone formation and the disruption of this coupling by currently approved antiresorptives (*e.g.* denosumab and bisphosphonates), the effect of Siglec-15-targeted therapies on bone formation is of great interest. Our examination of bone alkaline phosphatase staining in histological sections from Siglec-15 antibody-treated mice indicated that osteoblast activity is significantly increased. Likewise, the null mice generated by Hiruma *et al.* (27) displayed unchanged or moderately increased levels of osteocalcin, a bone formation biomarker. Kameda *et al.* (28) examined bone formation in their null mice by dynamic histomorphometry; notably, the mineral apposition rate was not affected in the secondary spongiosa and moderately decreased in the primary spongiosa of the *null* mice. Together, these results demonstrate that targeting osteoclasts via Siglec-15 does not lead to a dramatic decrease in bone formation, as typically observed with other anti-resorptive agents. It will be interesting to confirm in future studies whether the osteoclasts that are formed upon treatment with Siglec-15 antibodies continue to secrete factors that support osteoblasts.

Our results provide confirmation that Siglec-15 and DAP12 form a complex at endogenous expression levels in osteoclasts. Interestingly, mutations in DAP12 can cause a human condition, Nasu-Hakola disease, whose symptoms include bone lesions (30); in addition, DAP12-deficient mice exhibit osteopetrosis (31). An outstanding issue is why, despite the expression of DAP12 and its associated receptors in a range of hematopoietic cell types, DAP12 deficiency has such a prominent effect on bone (32). Our finding that targeting Siglec-15 has a similar impact on osteoclast function as DAP12 deficiency indicates that this highly osteoclast-specific complex is likely an important mediator of the physiological effects of DAP12.

[3] M. Stuible, A. Moraitis, A. Fortin, S. Saragosa, A. Kalbakji, M. Filion, and G. B. Tremblay, unpublished data.

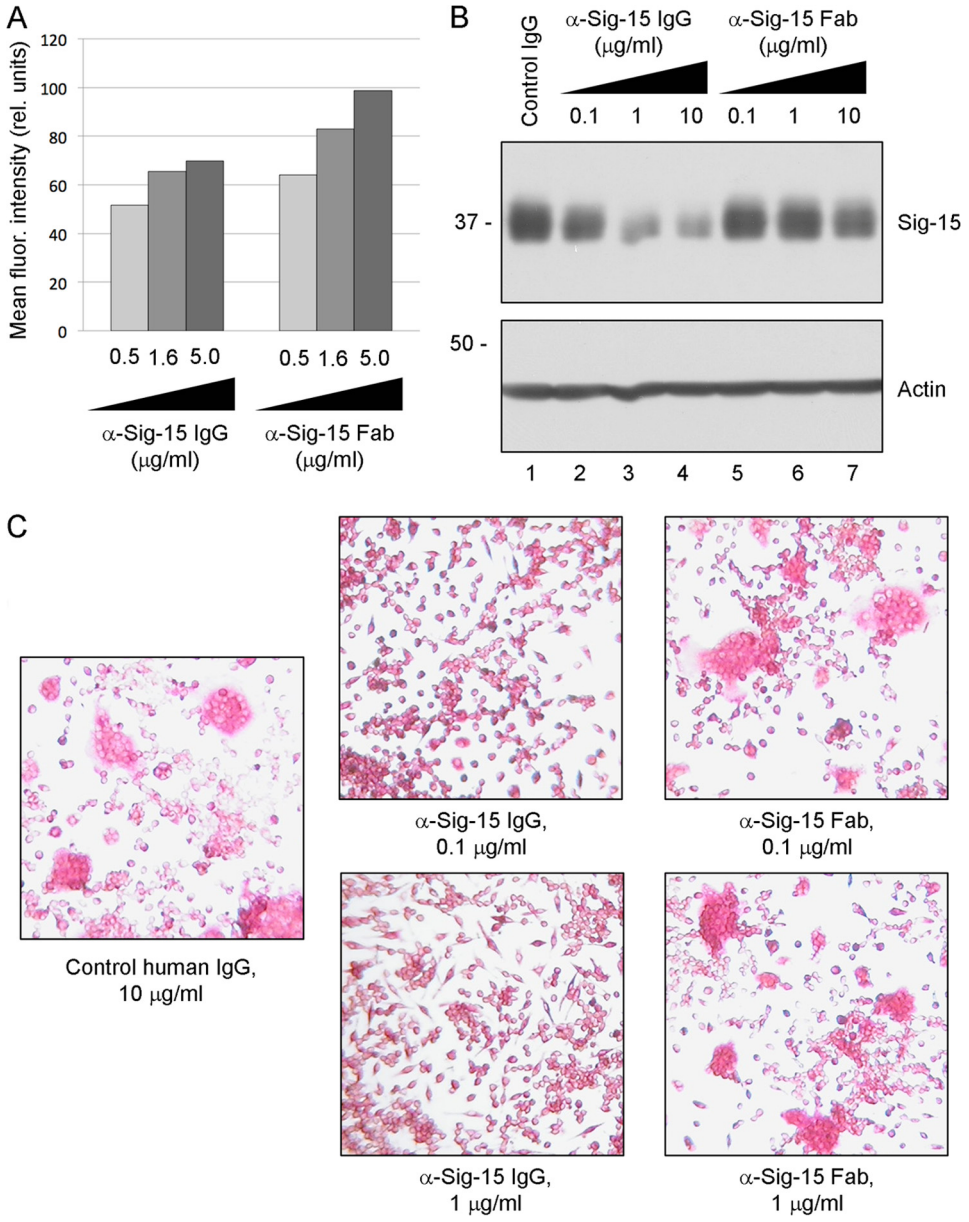

FIGURE 8. **Monovalent Fab fragments have reduced ability to induce degradation of Siglec-15 or inhibit osteoclast differentiation.** *A,* flow cytometry analysis of IgG/Fab binding to Siglec-15 expressed on intact cells. Full-length Siglec-15 was expressed in 2936E cells by transient transfection and cells were labeled with the indicated concentrations of anti-Siglec-15 B02 full IgG or Fab fragments. The values in the graph correspond to the mean fluorescence intensity of the transfected cells. *B,* RAW264.7-derived osteoclasts were treated with the indicated concentrations of anti-Siglec-15 B02 IgG or Fab or a control human IgG (10 μg/ml) for 2 h. Protein lysates were analyzed by Western blotting with the indicated antibodies. *C,* RAW264.7 cells were differentiated in the presence of the indicated IgG and Fab concentrations and stained for TRAP expression.

Considering the ability of DAP12 to mediate activation of multiple signaling pathways in different cellular contexts, the specificity of its effects downstream of Siglec-15 is remarkable. In particular, whereas DAP12 is tyrosine phosphorylated in response to Siglec-15 cross-linking and this is likely responsible for the concomitant activation of Akt, there is no effect on two other DAP12-associated signaling molecules, ERK and PLCγ. The p85 subunit of PI3K can be directly recruited to the DAP12 ITAM along with the kinase Syk, which is likely responsible for the robust activation of Akt that we detected (12). Syk and p85 are also capable of recruiting and activating ERK and PLCγ either directly or indirectly through scaffolding proteins LAT and NTAL, but this does not seem to occur in response to Siglec-15 clustering. The absence of PLCγ activation was surprising considering previous reports of the importance of a DAP12-dependent PLCγ costimulatory signal for the RANKL-induced up-regulation of NFATc1, a transcription factor that controls expression of numerous osteoclast-specific genes (33). Based on our results, we suspect that another DAP12-associated receptor, such as TREM2 (23), may be responsible for PLCγ activation and NFATc1 up-regulation early during osteoclast differentiation, whereas Siglec-15 may play a distinct role at a later stage, perhaps promoting osteoclast precursor fusion or functional maturation.

Following completion of the current study, Ishida-Kitagawa *et al.* (6) published a detailed analysis of the structural elements

of Siglec-15 required for osteoclastogenesis. The authors knocked down Siglec-15 expression in mouse bone marrow-derived macrophages, impairing their ability to differentiate into osteoclasts, and attempted to rescue this defect with various Siglec-15 mutants. As we suspected, a form of Siglec-15 lacking the DAP12-interacting transmembrane lysine residue was unable to rescue the defect like the WT protein. Interestingly, a fusion protein consisting of the extracellular and transmembrane domains of Siglec-15 and the cytoplasmic domain of DAP12 could restore osteoclast differentiation in this model, and this was dependent on tyrosine residues in the DAP12 ITAM motif. The authors also found that upon induction of DAP12 tyrosine phosphorylation by vitronectin stimulation, a complex containing Syk and Siglec-15 could be detected. These results support our hypothesis that Syk associates with Siglec-15 through DAP12 and contributes to downstream signaling, in particular the activation of Akt, and that this is important for osteoclastogenesis.

The activation of receptors at the cell surface and their endocytic down-regulation are often coupled as a means of limiting the intensity and duration of signaling. However, for Siglec-15, it seems that signaling and endocytosis occur exclusively of one another, depending on whether antibody ligation induces receptor clustering or simply dimerization. It is noteworthy that for other receptors that associate with DAP12 or the closely related adapter protein FcRγ, the avidity of the ligand-receptor interaction has been demonstrated to dictate signaling output: high-avidity ligands activate ITAM signaling (ERK, Akt, etc.), whereas low-avidity ligands promote recruitment of phosphatases that can inhibit these pathways (12). Our results suggest that another mechanism by which low-avidity ligands may inhibit receptor signaling is by promoting their endocytosis and lysosomal degradation.

Although its natural ligand is unknown, Siglec-15 has a preference for binding Neu5Acα2–6GalNAc glycans (14). Interestingly, formation of this type of glycan linkage is specifically important for osteoclast precursor fusion (34). We suspect that the Siglec-15 ligand is expressed on osteoclasts themselves, especially because Siglec-15 antibodies are effective in clonal RAW264.7 cultures, which lack any stromal cells or osteoblasts, which certainly do express other osteoclast-stimulatory factors (35). Notably, antibodies E09 and B02 do not seem to act by preventing Siglec-15-ligand binding: by ELISA, a polyclonal antibody can block binding of Siglec-15 to Neu5Acα2–6GalNAc, whereas E09 and B02 do not.[3] Instead, as outlined in Fig. 9, our data imply an alternative mechanism of action in which the antibodies induce Siglec-15 dimerization, leading to its endocytic down-regulation and degradation, thus indirectly preventing it from binding its ligand. The reduced activity of the B02 Fab fragment, which can still bind Siglec-15 but not promote its dimerization, further supports this hypothesis.

In summary, the present study contributes three important elements to our understanding of the biology of Siglec-15 and its usefulness as a therapeutic target. First, it provides further confirmation of the expression and functional importance of Siglec-15 in osteoclastogenesis. Second, our *in vivo* results demonstrate for the first time that Siglec-15 antibody can inhibit osteoclast activity in a physiological context and offer an exciting proof-of-principle for targeting Siglec-15 as a therapeutic strategy for bone loss. Finally, our analysis of Siglec-15-dependent signaling and antibody-induced receptor internalization has elucidated its cellular function as well as the mechanism of action of Siglec-15-targeted antibodies.

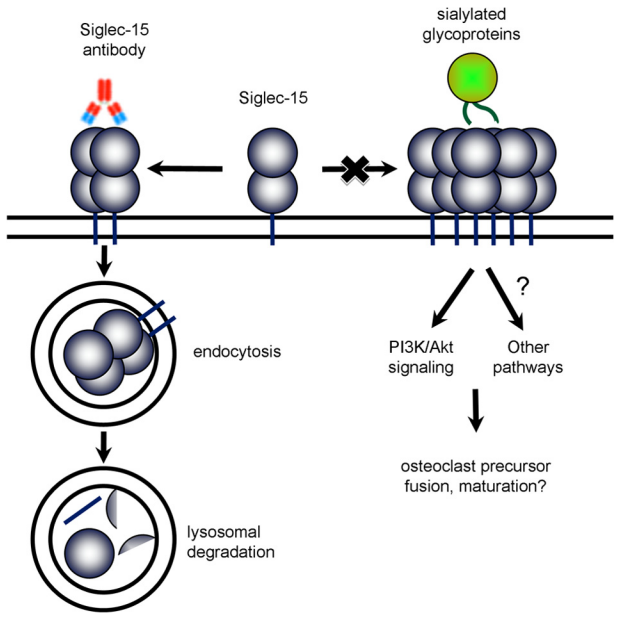

FIGURE 9. **Model of the mechanism of action of Siglec-15 antibodies on osteoclasts.** Siglec-15, by binding an unidentified sialo-glycoprotein ligand, is required for normal differentiation of functional osteoclasts. Siglec-15 ligands likely induce clustering of the receptor on the cell surface, leading to DAP12-dependent activation of Akt and possibly other pathways. Siglec-15 antibodies induce receptor internalization and degradation, effectively down-regulating Siglec-15 expression and preventing it from performing its essential signaling function.

The only currently approved antibody-based therapy for bone loss is denosumab, which targets the cytokine RANKL. Although its importance for osteoclastogenesis is unquestionable, RANKL exists in both membrane-associated and circulating forms that can affect a variety of tissue types and immune cells in addition to osteoclasts (36). In comparison, Siglec-15 is an osteoclast-intrinsic receptor with a highly restricted expression pattern, making it a favorable target with regards to specificity. It is also notable that although existing osteoclast-targeted therapies induce osteoclast cell death (bisphosphonates, (37)) or prevent their differentiation at an early stage (denosumab, (38)), Siglec-15 antibodies inhibit osteoclast differentiation at a relatively late stage. Thus, inhibiting Siglec-15 might preserve the coupled communication between osteoclasts and osteoblasts (35). This could potentially result in a reduction in the rare but devastating side effects of current therapeutics, which include osteonecrosis of the jaw (39), and atypical fractures of the femur (40). Both the specificity of Siglec-15 expression in osteoclasts and the potential for Siglec-15 targeted therapies to preserve osteoblast-osteoclast coupling and bone formation are supported by the mildly osteopetrotic but otherwise normal phenotype of the recently described *siglec-15*$^{-/-}$ mice (27, 28). Although further studies will be helpful to fully characterize their *in vivo* effects, these characteristics suggest that Siglec-15 antibodies could have distinct advantages over

existing drugs, and therefore, we believe that continued development of this novel class of bone loss therapeutic is certainly warranted.

Acknowledgments—We thank Dr. David Goltzman and Dr. William Boyle for reviewing the manuscript. We acknowledge the technical contributions of Émilie Turcotte and Dominique Bédard for the animal studies as well as Elisabeth Viau, Marc Sasseville, and Martine Pagé for production of the antibodies. We are also thankful to Denis Flipo from UQAM for assistance in confocal microscopy and the staff at the McGill Bone Centre for densitometry and microCT analyses. Anti-LAMP2 GL2A7 was obtained from the Developmental Studies Hybridoma Bank.

REFERENCES

1. Boyle, W. J., Simonet, W. S., and Lacey, D. L. (2003) Osteoclast differentiation and activation. *Nature* **423,** 337–342
2. Liu, Q. Y., Sooknanan, R. R., Malek, L. T., Ribecco-Lutkiewicz, M., Lei, J. X., Shen, H., Lach, B., Walker, P. R., Martin, J., and Sikorska, M. (2006) Novel subtractive transcription-based amplification of mRNA (STAR) method and its application in search of rare and differentially expressed genes in AD brains. *BMC Genomics* **7,** 286
3. Sooknanan, R. R., Tremblay, G. B., and Filion, M. (August 2, 2011) Polynucleotides and polypeptide sequences involved in the process of bone remodeling. Alethia Biotherapetuics, United States Patent 7,989,160
4. O'Reilly, M. K., and Paulson, J. C. (2009) Siglecs as targets for therapy in immune-cell-mediated disease. *Trends Pharmacol. Sci.* **30,** 240–248
5. Hiruma, Y., Hirai, T., and Tsuda, E. (2011) Siglec-15, a member of the sialic acid-binding lectin, is a novel regulator for osteoclast differentiation. *Biochem. Biophys. Res. Commun.* **409,** 424–429
6. Ishida-Kitagawa, N., Tanaka, K., Bao, X., Kimura, T., Miura, T., Kitaoka, Y., Hayashi, K., Sato, M., Maruoka, M., Ogawa, T., Miyoshi, J., and Takeya, T. (2012) Siglec-15 regulates the formation of functional osteoclasts in concert with DNAX-activating protein of 12 kDa (DAP12). *J. Biol. Chem.* **287,** 17493–17502
7. Crocker, P. R., Paulson, J. C., and Varki, A. (2007) Siglecs and their roles in the immune system. *Nat. Rev. Immunol.* **7,** 255–266
8. Law, C. L., Sidorenko, S. P., Chandran, K. A., Zhao, Z., Shen, S. H., Fischer, E. H., and Clark, E. A. (1996) CD22 associates with protein tyrosine phosphatase 1C, Syk, and phospholipase C-γ(1) upon B cell activation. *J. Exp. Med.* **183,** 547–560
9. Taylor, V. C., Buckley, C. D., Douglas, M., Cody, A. J., Simmons, D. L., and Freeman, S. D. (1999) The myeloid-specific sialic acid-binding receptor, CD33, associates with the protein-tyrosine phosphatases, SHP-1 and SHP-2. *J. Biol. Chem.* **274,** 11505–11512
10. Angata, T., Hayakawa, T., Yamanaka, M., Varki, A., and Nakamura, M. (2006) Discovery of Siglec-14, a novel sialic acid receptor undergoing concerted evolution with Siglec-5 in primates. *FASEB J.* **20,** 1964–1973
11. Blasius, A. L., Cella, M., Maldonado, J., Takai, T., and Colonna, M. (2006) Siglec-H is an IPC-specific receptor that modulates type I IFN secretion through DAP12. *Blood* **107,** 2474–2476
12. Turnbull, I. R., and Colonna, M. (2007) Activating and inhibitory functions of DAP12. *Nat. Rev. Immunol.* **7,** 155–161
13. Lanier, L. L. (2009) DAP10- and DAP12-associated receptors in innate immunity. *Immunol. Rev.* **227,** 150–160
14. Angata, T., Tabuchi, Y., Nakamura, K., and Nakamura, M. (2007) Siglec-15. An immune system Siglec conserved throughout vertebrate evolution. *Glycobiology* **17,** 838–846
15. Walker, J. A., and Smith, K. G. (2008) CD22. An inhibitory enigma. *Immunology* **123,** 314–325
16. Crocker, P. R., and Redelinghuys, P. (2008) Siglecs as positive and negative regulators of the immune system. *Biochem. Soc. Trans.* **36,** 1467–1471
17. Blasius, A. L., and Colonna, M. (2006) Sampling and signaling in plasmacytoid dendritic cells. The potential roles of Siglec-H. *Trends Immunol.* **27,** 255–260
18. Mühlbauer, R. C., Bauss, F., Schenk, R., Janner, M., Bosies, E., Strein, K., and Fleisch, H. (1991) BM 21.0955, a potent new bisphosphonate to inhibit bone resorption. *J. Bone Miner. Res.* **6,** 1003–1011
19. Egan, K. P., Brennan, T. A., and Pignolo, R. J. (2012) Bone histomorphometry using free and commonly available software. *Histopathology* **61,** 1168–1173
20. Dempster, D. W., Compston, J. E., Drezner, M. K., Glorieux, F. H., Kanis, J. A., Malluche, H., Meunier, P. J., Ott, S. M., Recker, R. R., and Parfitt, A. M. (2013) Standardized nomenclature, symbols, and units for bone histomorphometry. A 2012 update of the report of the ASBMR Histomorphometry Nomenclature Committee. *J. Bone Miner. Res.* **28,** 2–17
21. Kim, K., Lee, S. H., Ha Kim, J., Choi, Y., and Kim, N. (2008) NFATc1 induces osteoclast fusion via up-regulation of Atp6v0d2 and the dendritic cell-specific transmembrane protein (DC-STAMP). *Mol. Endocrinol.* **22,** 176–185
22. McHugh, K. P., Hodivala-Dilke, K., Zheng, M. H., Namba, N., Lam, J., Novack, D., Feng, X., Ross, F. P., Hynes, R. O., and Teitelbaum, S. L. (2000) Mice lacking β3 integrins are osteosclerotic because of dysfunctional osteoclasts. *J. Clin. Invest.* **105,** 433–440
23. Humphrey, M. B., Daws, M. R., Spusta, S. C., Niemi, E. C., Torchia, J. A., Lanier, L. L., Seaman, W. E., and Nakamura, M. C. (2006) TREM2, a DAP12-associated receptor, regulates osteoclast differentiation and function. *J. Bone Miner. Res.* **21,** 237–245
24. Underhill, D. M., and Goodridge, H. S. (2007) The many faces of ITAMs. *Trends Immunol.* **28,** 66–73
25. Bonifacino, J. S., and Traub, L. M. (2003) Signals for sorting of transmembrane proteins to endosomes and lysosomes. *Annu. Rev. Biochem.* **72,** 395–447
26. Toyomura, T., Murata, Y., Yamamoto, A., Oka, T., Sun-Wada, G. H., Wada, Y., and Futai, M. (2003) From lysosomes to the plasma membrane. Localization of vacuolar-type H^+-ATPase with the a3 isoform during osteoclast differentiation. *J. Biol. Chem.* **278,** 22023–22030
27. Hiruma, Y., Tsuda, E., Maeda, N., Okada, A., Kabasawa, N., Miyamoto, M., Hattori, H., and Fukuda, C. (2013) Impaired osteoclast differentiation and function and mild osteopetrosis development in Siglec-15-deficient mice. *Bone* **53,** 87–93
28. Kameda, Y., Takahata, M., Komatsu, M., Mikuni, S., Hatakeyama, S., Shimizu, T., Angata, T., Kinjo, M., Minami, A., and Iwasaki, N. (2013) Siglec-15 regulates osteoclast differentiation by modulating RANKL-induced phosphatidylinositol 3-kinase/Akt and Erk pathways in association with signaling adaptor DAP12. *J. Bone Miner. Res.* **28,** 2463–2475
29. Karsdal, M. A., Martin, T. J., Bollerslev, J., Christiansen, C., and Henriksen, K. (2007) Are nonresorbing osteoclasts sources of bone anabolic activity? *J. Bone Miner. Res.* **22,** 487–494
30. Paloneva, J., Kestilä, M., Wu, J., Salminen, A., Böhling, T., Ruotsalainen, V., Hakola, P., Bakker, A. B., Phillips, J. H., Pekkarinen, P., Lanier, L. L., Timonen, T., and Peltonen, L. (2000) Loss-of-function mutations in TYROBP (DAP12) result in a presenile dementia with bone cysts. *Nat. Genet.* **25,** 357–361
31. Kaifu, T., Nakahara, J., Inui, M., Mishima, K., Momiyama, T., Kaji, M., Sugahara, A., Koito, H., Ujike-Asai, A., Nakamura, A., Kanazawa, K., Tan-Takeuchi, K., Iwasaki, K., Yokoyama, W. M., Kudo, A., Fujiwara, M., Asou, H., and Takai, T. (2003) Osteopetrosis and thalamic hypomyelinosis with synaptic degeneration in DAP12-deficient mice. *J. Clin. Invest.* **111,** 323–332
32. Tomasello, E., and Vivier, E. (2005) KARAP/DAP12/TYROBP. Three names and a multiplicity of biological functions. *Eur. J. Immunol.* **35,** 1670–1677
33. Mao, D., Epple, H., Uthgenannt, B., Novack, D. V., and Faccio, R. (2006) PLCγ2 regulates osteoclastogenesis via its interaction with ITAM proteins and GAB2. *J. Clin. Invest.* **116,** 2869–2879
34. Takahata, M., Iwasaki, N., Nakagawa, H., Abe, Y., Watanabe, T., Ito, M., Majima, T., and Minami, A. (2007) Sialylation of cell surface glycoconjugates is essential for osteoclastogenesis. *Bone* **41,** 77–86
35. Raggatt, L. J., and Partridge, N. C. (2010) Cellular and molecular mechanisms of bone remodeling. *J. Biol. Chem.* **285,** 25103–25108
36. Walsh, M. C., and Choi, Y. (2003) Biology of the TRANCE axis. *Cytokine*

Growth Factor Rev. **14,** 251–263
37. Roelofs, A. J., Thompson, K., Gordon, S., and Rogers, M. J. (2006) Molecular mechanisms of action of bisphosphonates. Current status. *Clin. Cancer Res.* **12,** 6222s-6230s
38. Baron, R., Ferrari, S., and Russell, R. G. (2011) Denosumab and bisphosphonates. Different mechanisms of action and effects. *Bone* **48,** 677–692
39. Reid, I. R., and Cornish, J. (2012) Epidemiology and pathogenesis of osteonecrosis of the jaw. *Nat. Rev. Rheumatol.* **8,** 90–96
40. Park-Wyllie, L. Y., Mamdani, M. M., Juurlink, D. N., Hawker, G. A., Gunraj, N., Austin, P. C., Whelan, D. B., Weiler, P. J., and Laupacis, A. (2011) Bisphosphonate use and the risk of subtrochanteric or femoral shaft fractures in older women. *JAMA* **305,** 783–789